Defining the *p*-wave scattering volume in the presence of dipolar interactions

Anne Crubellier,[1,*] Rosario González-Férez,[2,†] Christiane P. Koch,[3,‡] and Eliane Luc-Koenig[1,§]

[1]*Laboratoire Aimé Cotton, CNRS, Université Paris-Sud, Université Paris-Saclay, ENS Paris-Saclay,*
Faculté des Sciences Bâtiment 505, 91405 Orsay Cedex, France
[2]*Instituto Carlos I de Física Teórica y Computacional and Departamento de Física Atómica, Molecular y Nuclear,*
Universidad de Granada, 18071 Granada, Spain
[3]*Theoretische Physik, Universität Kassel, Heinrich-Plett-Str. 40, 34132 Kassel, Germany*

The definition of the scattering volume for *p*-wave collisions needs to be generalized in the presence of dipolar interactions for which the potential decreases with the interparticle separation as $1/R^3$. Here, we propose a way to define the scattering volume characterizing the short-range interactions in odd-parity waves, by analyzing the *p*-wave component of the two-body threshold wave function. Our approach uses an asymptotic model and introduces explicitly the anisotropic dipole-dipole interaction, which governs the ultracold collision dynamics at long range. The short-range interactions, which are essential to describe threshold resonances, are taken into account by a single parameter related to the nodal structure of the wave functions at short distances.

I. INTRODUCTION

Collisions in ultracold atomic or molecular gases are universally described by the *s*-wave scattering length in case of bosons and unpolarized fermions or by the *p*-wave scattering volume in case of spin-polarized fermions. The value determines the strength of the interaction, which is repulsive (attractive) if the scattering length is positive (negative) [1]. Experimental control of the scattering properties, both scattering length and scattering volume, is a long-standing goal in ultracold gases [2–7].

Given the prominence of the elastic scattering parameters, it is somewhat unsatisfactory that all scattering parameters, even the scattering length, cannot be defined for an isotropic potential decreasing asymptotically as $1/R^3$ [8–11]. In detail, the tangent of the scattering phase shift at low energy cannot be expanded in powers of the wave number k of the incident wave. Simultaneously, the asymptotic threshold wave function includes an $\ln(R)$ contribution in addition to the $(R - a)$ term that defines the scattering length a. In contrast, for an anisotropic interaction decreasing as $1/R^3$, the *s*-wave scattering length is unambiguously defined. In this case, the effective *s*-wave potential decreases more rapidly, as $1/R^4$, which results in a "quasi-long-range" character of the dipole-dipole interaction [12,13]. In a previous study of non-resonant light control [14], we have verified this assertion by analyzing a particular threshold solution, the one that asymptotically decreases in all $\ell > 0$ channels while linearly increasing in the $\ell = 0$ channel. Here, we examine the definition of a *p*-wave scattering volume for an anisotropic $1/R^3$ interaction,

which is both an open problem and a prerequisite for studying nonresonant light control of *p*-wave scattering as discussed in the following paper, hereafter referred to as Paper II [15].

The paper is organized as follows. In Sec. II, we extend the standard definition of the scattering volume for two interacting ultracold atoms in the presence of nonresonant light. This field-dressed scattering volume is numerically determined in Sec. III, and we show that it presents a divergence each time a bound state appears at threshold. We conclude in Sec. IV.

II. SCATTERING VOLUME IN THE PRESENCE OF R^{-3} INTERACTION

In Sec. II A, we present the asymptotic Hamiltonian for a pair of particles in a nonresonant light and the reduced units suitable for describing the van der Waals interaction. For such a dipolar-like Hamiltonian, the scattering volume cannot be defined in the standard way (see Sec. II B). In Sec. II C, we disentangle the problem by considering a single-channel approximation in which the dominating channel coupling is accounted for through an adiabatic analytical *p*-wave potential. We then use an extension of the single-channel Levy-Keller approach [16] to determine analytically the scattering *p*-wave function that allows us to define the scattering volume. This function is written as a combination of two analytical reference functions, and the ratio between their amplitudes $\mathcal{M}(R)$ will turn out to be the key quantity for defining the scattering volume. Above the dissociation limit, when the spherical Bessel functions are used as reference functions, $\mathcal{M}(R)$ is identical to the tangent of the local *p*-wave phase of scattering theory (see Sec. II C). In Sec. II D, we consider the zero energy limit of $\mathcal{M}(R)$ and recall that for the potential decreasing asymptotically as $1/R^3$, $\mathcal{M}(R)$ takes for very large R a form including, aside from the standard term $\propto k^3$, a term linear in k, which prevents the use of the standard definition of the scattering volume. However, information on

*anne.crubellier@u-psud.fr
†rogonzal@ugr.es
‡christiane.koch@uni-kassel.de
§eliane.luc@u-psud.fr

the short-range interaction is captured by $\mathcal{M}(R)$ by restricting the analysis to the R range where kR is not too large. We show, in Sec. II E, that this restriction is equivalent to studying the asymptotic behavior of the threshold wave function using a pair of functions with asymptotic form $\sim R^2$ and $\sim 1/R$, a method frequently used in scattering theory. Then, the analytical expression of $\mathcal{M}(R)$ contains, aside from divergent asymptotic terms involving the multipolar parameters of the asymptotic potential, a constant term $\mathcal{M}_0$ depending on the short-range interactions only. This term $\mathcal{M}_0$ is identified as a scattering volume, and provides an extension of the standard definition.

A. Asymptotic Hamiltonian and reduced units

Within the Born-Oppenheimer approximation, the asymptotic Hamiltonian describing the relative nuclear motion of two atoms in a nonresonant light polarized along the laboratory Z axis reads as [14]

$$H = T_R + \frac{\hbar^2 \mathbf{L}^2}{2\mu R^2} + V_g(R) + \mathcal{D}\frac{3\cos^2\theta - 1}{R^3}, \qquad (1)$$

where R is the interparticle distance, μ the reduced mass, T_R the radial kinetic energy, and $\mathbf{L}$ the orbital angular momentum operator. The potential describing the short-range interaction $V_g(R)$ is limited here to the van der Waals potential $V_g(R) = -C_6/R^6$, with C_6 the van der Waals coefficient. The last term in the Hamiltonian Eq. (1) stands for the anisotropic interaction due to the coupling of the linearly polarized nonresonant light with intensity I and the polarizability anisotropy of the particles with strength

$$\mathcal{D} = \frac{4\pi I}{c}\alpha_1\alpha_2. \qquad (2)$$

Here, $\alpha_{1,2}$ are the static polarizabilities of the atoms and θ is the Euler angle between $\vec{R}$ and the Z axis. This is a dipole-dipole interaction, which also describes dipolar scattering of species with aligned permanent dipoles along the laboratory Z axis, either electric dipoles, such as found in polar heteronuclear molecules, or large magnetic dipole moments of ground-state open-shell atoms; cf. Paper II [15].

The Hamiltonian Eq. (1) commutes with parity and with the projection of the orbital angular momentum on the laboratory Z axis L_Z. As a result, the magnetic quantum number m and the parity are conserved.

A universal form of the Hamiltonian Eq. (1) is obtained by introducing reduced units. Here, we use the "van der Waals reduced units" (denoted as r.u.) with the reduced length x, energy $\mathcal{E}$, and nonresonant field intensity $\mathcal{I}$, respectively, defined by $R = \sigma x$, $E - E_0 = \epsilon \mathcal{E}$ (E_0 denotes the lowering of the dissociation limit), and $I = \beta \mathcal{I}$ [17,18]. The characteristic length σ, energy ϵ, and field intensity β are

$$\sigma = \left(\frac{2\mu C_6}{\hbar^2}\right)^{1/4}, \qquad (3a)$$

$$\epsilon = \frac{\hbar^2}{2\mu\sigma^2}, \qquad (3b)$$

$$\beta = \frac{c}{12\pi}\frac{\hbar^{3/2}C_6^{1/4}}{\alpha_1\alpha_2(2\mu)^{3/4}} = \frac{c\sigma^3\epsilon}{12\pi\alpha_1\alpha_2}. \qquad (3c)$$

These unit conversion factors contain all the information specific to the particle species (μ, C_6, α_1, and α_2). For a dipole-dipole interaction characterized by the strength $\mathcal{D}$ [Eq. (2)], the reduced intensity is $\mathcal{I} = 3\mathcal{D}/\epsilon\sigma^3$.

With these reduced units, the asymptotic Schrödinger equation associated to Hamiltonian Eq. (1) takes the form

$$\left[-\frac{d^2}{dx^2} + \frac{\mathbf{L}^2}{x^2} - \frac{1}{x^6} - \mathcal{I}\frac{\cos^2\theta - 1/3}{x^3} - \mathcal{E}\right]f(x,\theta,\phi) = 0, \qquad (4)$$

where $f(x,\theta,\phi)$ is the asymptotic wave function, x the interparticle separation, and (θ,ϕ) the Euler angles defining the orientation of the intermolecular axis in the laboratory fixed frame. For this anisotropic interaction, the total wave function $f(x,\theta,\phi)$ can be expanded in a conventional way into spherical harmonics (with a given parity and magnetic quantum number m owing to the symmetries of the Hamiltonian, and for practical reasons, a limited number of ℓ values), each multiplied by a radial function $u_\ell(x)$.

The field intensity $\mathcal{I}$ (in r.u.) is a tunable parameter allowing for the control of the collision. This has been discussed for even-parity ℓ states and $m = 0$, providing a means to tune the s-wave scattering length [14]. Here, we consider collisions in odd-parity states with $m = 0$ or ± 1.

B. Statement of the problem

In standard scattering theory, a first method to determine the scattering parameter in the channel ℓ consists in analyzing the asymptotic form of the radial component $u_\ell(x)$ of the multichannel solution of Eq. (4) at a vanishingly small positive energy. This function is written as a superposition of the regular $kx j_\ell(kx)$ and irregular $kx \eta_\ell(kx)$ spherical Bessel functions, where the latter is multiplied by $-\tan\delta_\ell(k,x)$, with $\delta_\ell(k,x)$ being the local phase converging at large distance, far from the potential barrier for $\ell \geqslant 1$, to the asymptotic phase shift $\delta_\ell(k)$, which is proportional to $k^{2\ell+1}$. The scattering parameter $(a_\ell)^{2\ell+1}$, which has the dimension of a length to the power of $(2\ell+1)$ and characterizes elastic collisions, is defined by the following low-energy limit:

$$\lim_{k\to 0} -\frac{\tan\delta_\ell(k)}{k^{2\ell+1}} = \frac{(a_\ell)^{2\ell+1}}{(2\ell+1)!!(2\ell-1)!!}. \qquad (5)$$

Notice that, with a potential decreasing as $1/x^q$, the limit in Eq. (5) does not exist for partial waves satisfying $\ell \geqslant (q-3)/2$ [8,19] because the tangent of the asymptotic phase shift increases as k^{q-2} independently of ℓ. Thus, the scattering volume for $\ell = 1$, i.e., $\mathcal{V} = (a_{\ell=1})^3/3$ (a factor of 3 is included to simplify further notation) is defined only for a potential decreasing asymptotically at least as $1/x^6$ [9]. As a consequence, the standard scattering volume is not defined for the $1/x^3$ dipole interaction appearing in Eq. (4).

A second standard method to calculate the scattering parameters $(a_\ell)^{2\ell+1}$ writes the asymptotic form of the zero energy wave function as a combination of the field-free regular $x^{\ell+1}$ and irregular $1/x^\ell$ spherical waves, the latter with a coefficient proportional to $-(a_\ell)^{2\ell+1}$ introduced in Eq. (5). For the slowly decreasing $1/x^3$ potential and $\ell = 1$, this standard scattering theory fails. Indeed, for very small

TABLE I. Effective potential [see Eq. (7)] in the p wave for a pair of atoms in a nonresonant light of intensity $\mathcal{I}$, given as a multipolar expansion with terms $-c_q/x^q$ ($3 \leqslant q \leqslant 6$). The c_q coefficients are reported for waves with magnetic quantum numbers $m = 0$ or $|m| = 1$. $V_d^m(x)$ is the diagonal term of the dipolar interaction (the diabatic potential). $V_{ad}^m(x)$ is the lowest eigenvalue of the two-channel Hamiltonian (adiabatic potential accounting in an effective way for the dominating dipolar couplings between the p and f channels). $V_{nad}^m(x)$ is the sum of the latter adiabatic potential and of the nonadiabatic coupling. Note that the $-c_3/x^3$ contribution is attractive for $m = 0$ and repulsive for $|m| = 1$.

V	$m = 0$				$|m| = 1$			
	c_3	c_4	c_5	c_6	c_3	c_4	c_5	c_6
V_d^m	$4\mathcal{I}/15$	0	0	1	$-2\mathcal{I}/15$	0	0	1
V_{ad}^m	$4\mathcal{I}/15$	$6\mathcal{I}^2/875$	$-4\mathcal{I}^3/65625$	$1 - 86\mathcal{I}^4/20671875$	$-2\mathcal{I}/15$	$4\mathcal{I}^2/875$	$8\mathcal{I}^3/65625$	$1 + 8\mathcal{I}^4/6890625$
V_{nad}^m	$4\mathcal{I}/15$	$33\mathcal{I}^2/4375$	$-4\mathcal{I}^3/46875$	$1 - 3814\mathcal{I}^4/516796875$	$-2\mathcal{I}/15$	$22\mathcal{I}^2/4375$	$8\mathcal{I}^3/46875$	$1 + 472\mathcal{I}^4/172265625$

k, $\tan \delta_{\ell=1}(k, x)$ tends to a limit proportional to k. Simultaneously, writing the asymptotic form of the threshold wave function as $x^2 - (a_{\ell=1}(x))^3/3x$, the term $(a_{\ell=1}(x))^3$ diverges for $x \to \infty$ according to Eq. (5). Searching for a quantity characterizing the nonuniversal part of the near threshold dipolar scattering, i.e., a signature of the contribution of the short-range interactions, we show that one can study the behavior of the local phase for $k \to 0$ and $x \to \infty$ while keeping xk finite, i.e., for intermediate distances x such that the energy remains well below the potential barrier. This is equivalent, in the study of the threshold wave function, to determine the asymptotically divergent contributions to $(a_{\ell=1}(x))^3$ and to eliminate them. This strategy is used in the following section.

C. Effective *p*-wave potential and Levy-Keller wave function

We start by introducing a single-channel approximation, accounting in an effective way for the dominating dipolar couplings between the lowest odd partial ℓ waves, which prevail close to threshold at least for not too strong dipolar coupling. We describe analytically the effective ℓ-dependent potential by its asymptotic multipolar expansion

$$V_\ell(x) = -\frac{c_3^\ell}{x^3} - \frac{c_4^\ell}{x^4} - \frac{c_5^\ell}{x^5} - \frac{c_6^\ell}{x^6}. \qquad (6)$$

The dipole-dipole interaction in Eq. (4) directly couples the ℓ and $\ell \pm 2$ channels. As a consequence, the contribution of the $\ell = 1 + 2q$ channel to the p-wave effective potential in Eq. (6) appears at order q of perturbation theory and increases as $\mathcal{I}^q/x^{q+2}$.

We use the three different effective potentials given in Table I to approximate the multipolar expansion in Eq. (6). The simplest one is the diabatic potential $V_d^m(x)$, which is equal to the $\ell = 1$ diagonal matrix element in the spherical harmonic representation of the potential in Eq. (4). If the coupling between ℓ and $\ell \pm 2$ channels is not small compared to the diagonal terms, it is advantageous to introduce an adiabaticlike representation restricted to the $\ell = 1$ and 3 channels for which an analytical formulation remains tractable. The second approximation is thus the effective adiabatic potential $V_{ad}^m(x)$ (see Table I), which is the lowest eigenvalue of the 2×2 potential matrix accounting for the coupling between the $\ell = 1$ and 3 channels. The third one is the $V_{nad}^m(x)$ potential, and adds to $V_{ad}^m(x)$ the diagonal contribution of the nonadiabatic coupling arising from the x dependence of the adiabatic eigenvector $\Psi(x)$, the so-called "kinetic energy"

term $\langle \Psi \,|\, d^2\Psi/dx^2 \rangle$. For the considered range of intensities $\mathcal{I} < 40$ r.u., $V_{nad}^m(x)$ with multipolar coefficients up to $q = 6$ describes rather well the effective potential in the p wave at distances $x > 20$ r.u.

For each partial ℓ wave and energy $\epsilon = k^2 \geqslant 0$, the radial Schrödinger equation

$$u_\ell''(x) - \left[\frac{\ell(\ell+1)}{x^2} + V_\ell(x) + k^2 \right] u_\ell(x) = 0 \qquad (7)$$

can be solved analytically either exactly or using perturbation theory. For simplicity, the ℓ dependence of $V_\ell(x)$, the coefficients c_i^ℓ and $u_\ell(x)$ are omitted in the rest of this section.

The two-potential Levy-Keller method [16,20], which is described in Appendix A 1, constructs the solution of the radial Schrödinger Eq. (7) as the following linear combination of two reference functions $(\varphi(x), \psi(x))$:

$$u(x) = \mathcal{A}(x)(\varphi(x) - \psi(x)\,\mathcal{M}(x)). \qquad (8)$$

These reference functions $(\varphi(x), \psi(x))$ are solutions of the Schrödinger Eq. (7) at the same energy as $u(x)$ but for the potential $V_f(x) = -c_{pf}/x^q$, the dominant term in $V(x)$. Thus, $V_f(x)$ is a zeroth-order approximation to $V(x)$, and, as a consequence, $u(x)$ in Eq. (7) is a very rough approximation of the radial ℓ-wave component of the multichannel solution $f(x, \theta, \phi)$ in Eq. (4).

The function $\mathcal{M}(x)$ in Eq. (8) satisfies the nonlinear first-order differential Eq. (A2a), and the logarithmic derivative of $\mathcal{A}(x)$ the first-order differential Eq. (A2b) involving $\mathcal{M}(x)$. Each of these differential Eqs. (A2a) and (A2b) introduces a single integration constant $\mathcal{M}_0$ and $\mathcal{A}_0$, respectively. $\mathcal{A}_0$ is a global multiplicative constant without interest here, whereas $\mathcal{M}_0$ is an additive constant. We show below that $\mathcal{M}_0$ characterizes the short-range nonuniversal contributions to the dipolar scattering, and can be identified as the scattering volume. This is in line with $\mathcal{M}(x)$ in $u(x)$ Eq. (8) taking the role of the tangent of a local phase, apart from the fact that for the presently studied dipolar interaction this function does not tend to a limit as x increases.

In this work, we define reference pairs for either k small and positive or $k = 0$ using three analytical potentials $V_f(x)$. Details on these reference pairs are given in Table II and in Appendix A 2. For $k > 0$, we take $V_f(x) = 0$ and the resulting reference pair $(\varphi(x), \psi(x))$, labeled as BC2k, corresponds to free partial spherical waves. For $k = 0$, we consider either the pair $(x^{\ell+1}, 1/x^\ell)$, labeled as BC2, corresponding to the

TABLE II. Analytical expressions of the reference pairs labeled in column 1. Van der Waals reduced units r.u. defined in Sec. II B are used. The linearly independent functions $(\varphi(x), \psi(x))$, which are ℓ-wave solutions of the Schrödinger equation of the potential $V_f(x)$ at energy $\epsilon = k^2$ (k specified in column 2), are presented in the first and second lines of column 3, and their Wronskian W in column 5. The BC2k functions are free spherical waves [$V_f(x) = 0$] at positive energy $k > 0$. The BC2 and BC23 functions are spherical solutions at threshold $k = 0$ of $V_f(x) = 0$ and $V_f(x) = -c_{3f}/x^3$ with $c_{3f} > 0$, respectively. The asymptotic limits of these functions are given in the fourth column, note that the free spherical waves at threshold (BC2) are equal everywhere to their asymptotic form. The analytical functions BC23 are given in Ref. [31].

Label	k	Pair of functions	Asymptotic limits	W
BC2k	>0	$kx\, j_\ell(kx)$	$\sin(kx - \ell\pi/2)$	$-k$
		$-kx\, \eta_\ell(kx)$	$-\cos(kx - \ell\pi/2)$	
BC2	0	$x^{\ell+1}$	$x^{\ell+1}$	$-(2\ell+1)$
		$x^{-\ell}$	$x^{-\ell}$	
BC23	0	$-\pi\, (c_{3f})^{\ell+1/2}/(2\ell)!\, \sqrt{x}\, Y_{2\ell+1}(\sqrt{4c_{3f}/x})$	$x^{\ell+1}$	$-(2\ell+1)$
		$(c_{3f})^{-\ell-1/2}\, (2\ell+1)!\sqrt{x}\, J_{2\ell+1}(\sqrt{4c_{3f}/x})$	$x^{-\ell}$	

spherical solution at threshold of the free motion, or the BC23 pair, which is solution at threshold of $V_f(x) = -c_{3f}/x^3$. The $\ell = 1$ reference functions $\varphi(x)$ and $\psi(x)$ vary as x^2 and $1/x$, everywhere for the BC2 pair and when $x \to \infty$ for the BC23 functions. The same behavior occurs for the BC2k reference pair in the x range satisfying kx small. In all three cases, $\mathcal{M}(x)$ represents (in reduced units) a quantity that has dimension of volume.

Using these reference functions, we determine analytical expressions for the asymptotic behavior of $\mathcal{M}(x)$ depending on the coefficients of the multipolar expansion in Eq. (6) of the effective single-channel p-wave potential (see Appendix A 3). Using these coefficients given in Table I, the derivation of the asymptotic behavior of $\mathcal{M}(x)$ numerically calculated in multichannel models (see Sec. III and Appendix B) becomes tractable. In particular, it allows us to justify the procedure developed in Sec. III A to extract from $\mathcal{M}(x)$ a constant term similar to $\mathcal{M}_0$, characterizing the interactions at short range, and defining a scattering volume.

D. Evaluating the $k \to 0_+$ limits for large kx: Universal behavior

The scattering parameters are determined at very low positive energy $k \to 0_+$ in the limit $x \to \infty$ [see Eq. (5)]. We first show that the standard way cannot be used to define the scattering volume in the presence of an isotropic potential decreasing as $1/x^3$.

Following the two-potential approach [20], we consider a potential consisting of a short-range part which vanishes for $x > d$ and, therefore, gives rise to the short-range phase shift $t_0 = \tan[\delta_{\ell=1}(k, x = d)]$ approximated close to threshold by its leading term $t_0 \sim -A\, k^3$ and of a long-ranged part vanishing for $x < d$ while identical to $-c_3/x^3$ for $x > d$. The asymptotic p-wave phase shift $\tan\delta_{\ell=1}(k) = \lim_{x\to\infty} \mathcal{M}(x)$ is calculated by using the Levy-Keller approach to first order of the perturbation theory, by using the reference functions BC2k [$V_f(x) = 0$] (see Table II) and by setting $\mathcal{M}(x) \equiv t_0$ in the right-hand side of the Ricatti equation [Eq. (A2a)]. The integrals occurring in $d\mathcal{M}(x)/dx$ involve the regular [$\varphi(x)$] and/or irregular [$\psi(x)$] spherical Bessel functions and are analytically evaluated [20,21]. There is no contribution from the upper integration limit ($kx \to +\infty$) in these integrals and from the lower limit (kd small for sufficiently small k) one

obtains at low energy

$$\tan\delta_{\ell=1}(k) \sim k\frac{c_3}{4} - k^3\left(A - \frac{c_3 A^2}{4d^4} + \frac{2Ac_3}{3d} + \frac{c_3 d^2}{18}\right)\ldots. \tag{9}$$

This expression is identical to the one of Ref. [21] disregarding the effective range contribution to t_0. The term linear in k is identical to the one obtained in the treatment of the potential $-c_3/x^3$ in the Born approximation [22]. Note that it is the $\propto 1/x^3$ potential, which is at the origin of the contribution linear in k in the asymptotic phase shift but this contribution does not contain any contribution arising from the short-range interactions. When k tends to zero and x tends to infinity, kx becoming infinite, the tangent of the phase shift converges to $\tan\delta_\ell(k) \propto k\, c_3$ for all the partial waves with $\ell \geqslant 1$. Due to the linear term, $\tan\delta_{\ell=1}(k)/k^3$ obviously diverges for $k \to 0_+$ and the scattering volume cannot be defined in the standard way. The elastic partial cross sections $\propto (\sin\delta_\ell(k)/k)^2$ become independent of the collision energy at very low temperature and depend on the square of the strength of the dipolar interaction only, which is the so-called "universal" behavior [10,11,23]. Let us mention that the low-k expansion of the partial-wave dipolar phase shifts $\delta_{\ell,m}(k)$ for $\ell \geqslant 1$ to orders k^p higher than the leading order $p = 1$ have been studied in a multichannel treatment [24], giving, for the coefficients, some insight in the universal scaling laws on the strength of the coupling $\propto \mathcal{D}^q$ [Eq. (2)] as well as in their nonuniversal contributions.

For a given species, the specific (nonuniversal) short-range part of the potential can manifest itself by the existence of shape resonances, not accounted for by the Born approximation, while already present in the short-range phase t_0 (or A) [Eq. (9)]. These resonances appear for particular short-range properties and in a specific energy domain fixed by the rotational barrier height, which depends on the magnetic quantum number m and on the dipolar interaction strength. In Sec. III B, we define from the threshold wave function a scattering volume depending also on m, on the dipolar interaction strength, and, in addition, on the short-range interactions. This scattering volume presents divergences whose position and width give the domain where shape resonances can be expected.

E. Defining the scattering volume via the threshold wave function

Just above threshold ($k \to 0_+$) and for intermediate values of x such that kx remains very small, the BC2k reference functions of $\ell = 1$ wave used in previous section II D can be replaced by their leading terms $\varphi(x) \approx (kx)^2/3$ and $\psi(x) \approx 1/(kx)$ (see Table II). Inserting this approximation into the differential Eq. (A2a) for $\mathcal{M}(x)$, and setting $\overline{\mathcal{M}}(x) = 3\mathcal{M}(x)/k^3$, we obtain

$$\frac{d\overline{\mathcal{M}}(x)}{dx} = -\frac{c_3}{3\,x^3}\left(x^2 - \frac{\overline{\mathcal{M}}(x)}{x}\right). \quad (10)$$

Using the BC2 reference functions (free spherical *p*-wave functions at threshold) $\varphi_{\text{BC2}}(x) = x^2$ and $\psi_{\text{BC2}}(x) = 1/x$ in the Levy-Keller approach, $\mathcal{M}(x)$ is solution of Eq. (10). Thus, in the limited x range where kx remains small, the relative amplitude $\mathcal{M}(x)$ obtained with the BC2k pair just above threshold is identical to that obtained at threshold using the BC2 pair. This has been numerically verified for various light intensities, for energy and x values verifying $0.01 \leqslant kx \leqslant 0.1$. Therefore, we will characterize the low-energy *p*-wave dipolar scattering by the threshold wave functions, more precisely by the quantities $\mathcal{M}(x)$ and $\mathcal{A}(x)$ determined for the BC2 reference pair.

To obtain an analytical asymptotic expression for the solution of Eq. (A2a), we expand $\mathcal{M}(x)$ into terms $1/x^q$ (with $q \geqslant -2$) and $\ln(x)/x^q$ with ($q \geqslant 0$), therefore including the asymptotic divergent terms x^2, x, and $\ln(x)$. We determine the coefficients of this expansion by equating the corresponding terms on both sides of the equation. For the BC2 and BC23 reference functions, the results are reported in Eqs. (A3) and (A4), respectively. In the expansions in Eqs. (A3) and (A4), this method allows for the determination of all coefficients, except the integration constant $\mathcal{M}_0$ of the Ricatti equation [Eq. (A2a)], which may depend on the reference pair. The other coefficients in the expansion of $\mathcal{M}(x)$ express in terms of the multipolar coefficients c_p of the long-range potential $V(x)$, on c_{3f} defining the single-term potential $V_f(x)$, and also on the integration constant $\mathcal{M}_0$.

Using the $\mathcal{M}(x)$ expansions up to the order $1/x^7$, we integrate the first-order differential Eq. (A2b) for the logarithmic derivative of $\mathcal{A}(x)$. The integration constant $\mathcal{A}_0$ is determined by imposing the condition $u(x) \to x^2$ for $x \to \infty$ upon the threshold wave function, which implies $\mathcal{A}(x) \to 1$. For the BC2 and BC23 reference pairs, the expressions of $\mathcal{A}(x)$ are given in Eqs. (A5) and (A6), respectively, and the corresponding threshold wave functions $u(x)$ in Eqs. (A7) and (A8).

The parameter $\mathcal{M}_0$ does not depend on the asymptotic form of the potential and accounts for the interactions at short range. Since $\mathcal{M}_0$ is the value in reduced units of a quantity that has dimension of volume, it is a good candidate for defining a scattering volume, except for its dependence on the chosen reference functions. We show next that in fact $\mathcal{M}_0^{\text{BC2}}$ and $\mathcal{M}_0^{\text{BC23}}$ provide equivalent descriptions of the short-range interactions. Indeed, the threshold wave function does not depend on the choice of the reference pair and equalizing the coefficients of the $1/x^q$ and $\ln(x)/x^q$ terms in the expansions BC2 [Eq. (A7)] and BC23 [Eq. (A8)] of $u(x)$ leads to the following unique relation:

$$\mathcal{M}_0^{\text{BC23}} - \mathcal{M}_0^{\text{BC2}} = -\frac{2}{9}c_{3f}c_4 - \frac{11}{144}c_3^2 c_{3f} - \frac{1}{24}c_3 c_{3f}^2$$
$$+ \left(\frac{83}{432} - \frac{\gamma}{6} - \frac{\ln(c_{3f})}{12}\right)c_{3f}^3, \quad (11)$$

where γ denotes the Euler constant. Note that we have verified the uniqueness of this relation (11) for terms up to $q = 5$. The difference $\Delta\mathcal{M}_0 = \mathcal{M}_0^{\text{BC23}} - \mathcal{M}_0^{\text{BC2}}$ depends on the parameters c_3, c_4, and c_{3f}, and is perfectly known as soon as the reference pairs are chosen. Therefore, it is sufficient to determine $\mathcal{M}_0^{\text{BC2}}$ because $\mathcal{M}_0^{\text{BC23}}$ is known unambiguously once c_{3f} is fixed. In particular, $\mathcal{M}_0^{\text{BC23}}$ and $\mathcal{M}_0^{\text{BC2}}$ diverge simultaneously. The divergences, the most important features in scattering, indicate a quasiresonant situation with a bound state located just at threshold, which can lead to the observation of a threshold resonance in the cross section. They are associated to infinite contact interactions in a pseudopotential technique describing the short-range interaction of the two particles by ℓ-wave contact potentials [25,26].

So far, analytic solutions at threshold are derived in a single-channel approximation in Eq. (7) of the coupled-channels asymptotic Schrödinger Eq. (4). The coefficients of the analytical single-channel Levy-Keller formula are evaluated by using the effective adiabatic potential in the *p*-wave Table I. These results are used in Sec. III A to analyze the asymptotic behavior of $\mathcal{M}(x)$ calculated in multichannel models. This allows us to justify the procedure developed below to extract from $\mathcal{M}(x)$ a constant term similar to $\mathcal{M}_0$ occurring in the Levy-Keller approach and characterizing the interactions at short range.

III. DETERMINING THE SCATTERING VOLUME FROM MULTICHANNEL ASYMPTOTIC CALCULATIONS

In this section, we describe how to determine the field-dressed scattering volume $\mathcal{M}_0$ in the multichannel case. We use an asymptotic model and the nodal line technique [14], reviewed briefly in Appendix B 1. All the calculations are restricted to the asymptotic Hamiltonian, which is valid for $x \geqslant x_{00}$, and accounts for the van der Waals and dipolar interactions. All the short-range physics, specific to each collision pair, is replaced by boundary conditions in all partial waves depending on a single parameter x_{00} called the nodal parameter. x_{00} is the position of one of the most outer nodes of the field-free *s*-wave function at threshold. The knowledge of x_{00} is equivalent to knowing the *s*-wave scattering length. Note that the positions of the nodes in the inner region where the van der Waals interaction dominates are quasiperiodic with almost the same period for different ℓ. It is therefore sufficient to choose one period for the *s*-wave node position in order to span all values of the scattering parameter a_ℓ in Eq. (5) for all ℓ. The nodal parameter determines the position of the ℓ-, energy-, and field-intensity-dependent nodal lines used in our universal model [17,18].

In Sec. III A, we describe the calculation of $\mathcal{M}(x)$, the tangent of the local phase, that we expand in an analytical form involving the x-dependent terms suggested by the single-channel Levy-Keller approach. A numerical fitting procedure

allows us to extract from $\mathcal{M}(x)$ a constant similar to $\mathcal{M}_0$ occurring in the single-channel model (see Sec. II E). This constant depends only on the short-range interactions, i.e., on the nodal parameter x_{00}, and is identified as the field-dressed scattering volume. A detailed comparison of the numerical multichannel results with the analytical single-channel Levy-Keller ones justifies the procedure used to calculate this scattering volume $\mathcal{M}_0$. In Sec. III B, we show that its dependence on the field-free scattering length, equivalently on the nodal parameter x_{00}, displays a divergence each time a bound state is located at threshold. A similar resonance structure occurs when the nonresonant light intensity varies.

A. Asymptotic behavior of $\mathcal{M}(x)$ from numerical calculations

We start with a short description of the method used to determine the asymptotic behavior of $\mathcal{M}(x)$ (see Appendix B 1 for more details). For a chosen pair of colliding partners, i.e., a fixed nodal parameter, a given dipolar interaction strength $\mathcal{D}$ [Eq. (2)], a given magnetic quantum number m, and, for practical reasons, a limited number of ℓ values, we calculate by inward integration a complete set of physical solutions of the threshold Schrödinger Eq. (4) for a chosen starting point $x_{\max}$ of the integration procedure. We start by calculating particular solutions, for which short-range boundary conditions are not yet included, while the chosen analytic asymptotic form of the solutions determines the initial conditions for the integration. More precisely, at $x_{\max}$ all but one radial components vanish, except in a particular channel ℓ where they are equal to the BC2 or the BC23 functions (see Table II). The number of particular solutions with diverging and nondiverging asymptotic behavior is twice the number of physical solutions, i.e., the number of ℓ channels included in the calculation. The physical solutions are constructed as linear combinations of the particular solutions with coefficients determined by imposing the short-range boundary conditions, i.e., by the canceling of all radial components on the nodal lines defined by the nodal parameter x_{00}.

We then focus on the specific physical solution with a large radial component at $x_{\max}$ only in the channel $\ell = 1$. At the starting point $x_{\max}$, its radial p component is a linear combination of the diverging and converging reference functions, with factors 1 and $-\mathcal{M}(x_{\max})$, respectively, as in the single p-channel model in expression of Eq. (8). The boundary conditions on the nodal line allow us to determine $\mathcal{M}(x)$ at $x_{\max}$. By performing several calculations with different starting points $x_{\max}$, we obtain $\mathcal{M}(x)$. We assume that $\mathcal{M}(x)$ can be expanded in an analytical form involving the terms suggested by the single-channel Levy-Keller approach [cf. Eqs. (A3) and (A4)]. For the initial condition BC2, we consider the following terms:

$$x^2,\ x,\ \ln(x),\ 1,\ \frac{\ln(x)}{x},\ \frac{1}{x},\ \frac{\ln(x)}{x^2},\ \frac{1}{x^2},\ \ldots . \quad (12a)$$

For $|m| = 1$, choosing $c_{3f} = |c_3|$ in the initial condition BC23, we have the same terms as for BC2, whereas for $m = 0$ and choosing $c_{3f} = c_3$ in BC23, we have the following terms:

$$x,\ \ln(x),\ 1,\ \frac{1}{x},\ \frac{\ln(x)}{x^2},\ \frac{1}{x^2},\ \ldots . \quad (12b)$$

Finally, we perform a fitting procedure in $x_{\max}$, the range of $x_{\max}$ being adapted to this fitting procedure and spanning a large domain where the dipolar interaction prevails, typically 20 r.u. $\leqslant x_{\max} \leqslant 500$ r.u.. For the typical systems analyzed in Paper II (see Tables I and II of Ref. [15]), the characteristic lengths of the van der Waals and dipolar interactions, which are equal for $\mathcal{I} = 6$ r.u., amount to $\sigma \sim 150\,a_0$, and the resulting $x_{\max}$ interval is $[3000\,a_0, 75\,000\,a_0]$. The fits allow us to extract from $\mathcal{M}(x)$ a constant similar to $\mathcal{M}_0$ occurring in the single-channel model in Sec. II E. This constant, which depends only on the short-range interactions, i.e., on the nodal parameter x_{00}, is identified as the field-dressed scattering volume.

For $m = 0$ and ± 1, $\mathcal{M}(x_{\max})$ has been computed using $n = 3$ channels with $\ell = 1, 3, 5$, three intensities $\mathcal{I}$, and $0.142\,152$ r.u. $\leqslant x_{00} \leqslant 0.152\,135$ r.u., the field-free scattering length, quasiperiodic function of x_{00}, varying from $-\infty$ to $+\infty$ in this interval. The inward integration has been initialized with the BC2 and BC23 boundary conditions (see Table II), and $x_{\max}$ is varied in the range $[20, 500]$ r.u. The numerical coefficients of the $\mathcal{M}(x_{\max})$ fits are reported in Table III. For fixed m, $\mathcal{I}$, and BC conditions, some coefficients are independent of x_{00}, whereas others depend on x_{00}. The x_{00}-independent coefficients have been compared to the analytical ones deduced from the single-channel Levy-Keller approach using the multipolar coefficients c_p of the adiabatic p-wave potential $V_{\text{nad}}^m(x)$, given in Table I and the c_{3f} coefficient for the BC23 boundary condition. We find good agreement between the numerical and analytical results. The x_{00}-dependent coefficients, labeled as $v_m(\mathcal{I}, x_{00})$ and $\eta_m(\mathcal{I}, x_{00})$, are the prefactors of the constant and $1/x$ terms, respectively. They display the same characteristic x_{00} dependence with several divergences. In fact, as expected from the Levy-Keller approach [see Eqs. (A3) and (A4)], these coefficients are related as $\eta_m(\mathcal{I}, x_{00}) = \alpha \times v_m(\mathcal{I}, x_{00}) - \beta$, with α and β independent of x_{00} and expressing analytically in terms of the c_p and c_{3f} coefficients only. Here also the numerically obtained coefficients α and β are x_{00} independent and agree with the analytical ones. For given m and $\mathcal{I}$, the curves $v_m(\mathcal{I}, x_{00})$ associated to the constant term of the expansion and obtained with the BC2 and BC23 reference functions differ by a quantity that does not depend on x_{00}. The numerical value of this difference is in good agreement with the analytical formula $\Delta \mathcal{M}^0 = \mathcal{M}_{\text{BC23}}^0 - \mathcal{M}_{\text{BC23}}^0$ [Eq. (11)] calculated using the c_p and c_{3f} coefficients.

We can also interpret satisfactorily the coefficients of the $\mathcal{M}(x)$ asymptotic expansion from the multichannel calculations by comparison with the $\mathcal{M}(x)$ expansion deduced from the analytical single-channel Levy-Keller approach. In detail, we use the coefficients of the adiabatic p-wave potential (see Table I) and the asymptotic boundary conditions deduced from the potential $V_f(x)$ introduced in the Levy-Keller approach (see Appendix A 1). This comparison justifies the identification of the constant term $v_m(\mathcal{I}, x_{00})$ of this multichannel calculation with the field-dressed scattering volume. By analogy to the definition deduced from the single-channel Levy-Keller approach, the label $\mathcal{M}_0(\mathcal{I}, x_{00})$ is introduced instead of $v_m(\mathcal{I}, x_{00})$.

The fairly good agreement between the coefficients of the $\mathcal{M}(x)$ expansion according to Eq. (12) obtained from the

TABLE III. The table presents the first coefficients of the expansion of $\mathcal{M}(x_{max})$ in powers of $1/x_{max}$, obtained by a fit performed with x_{max} spanning the interval [20 r.u., 500 r.u.]. The nonresonant light intensity $\mathcal{I}$, the magnetic quantum number m, and the asymptotic boundary conditions BC are specified in columns 1, 2, and 3, respectively. The intensity dependence of the coefficients is indicated below the coefficients in the second line of the top cells. The numerical calculations of $\mathcal{M}(x_{max})$ include three coupled channels $\ell = 1, 3, 5$ using 150 or 200 values of the nodal parameter x_{00}, chosen such that the field-free *s*-wave scattering length varies from $-\infty$ to $+\infty$. For given $\mathcal{I}$, m, and BC, and for each value of x_{00}, the calculated function $\mathcal{M}(x_{max})$ is fitted to the analytic expansions in Eq. (12). In each cell of cell lines 2 to 13 and columns 4 to 11, the first line reports either the numerical values of the coefficients of the terms, when it does not vary with x_{00}, or the symbol $v(\mathcal{I}, x_{00})$ or $\eta(\mathcal{I}, x_{00})$ for the x_{00}-dependent ones. The second line gives the analytical results obtained with the Levy-Keller formulas in Eqs. (A3) and (A4), for the single channel $\ell = 1$ and for the potential $V_{nad}^m(x)$ (Table I). Except for the BC23 reference pair and $m = 0$, the coefficients $v_m(\mathcal{I}, x_{00})$ and $\eta_m(\mathcal{I}, x_{00})$ are related by a linear transformation $\eta(\mathcal{I}, x_{00}) = v(\mathcal{I}, x_{00}) \times \alpha - \beta$, in Eqs. (A3) and (A4). All data are in reduced units.

$\mathcal{I}$	m	BC	$\dfrac{x_{max}^2}{\mathcal{I}}$	$\dfrac{x_{max}}{\mathcal{I}^2}$	$\dfrac{\ln(x_{max})}{\mathcal{I}^3}$	Constant	$\ln(x_{max})/x_{max}$ $\mathcal{I}^4$	$1/x_{max}$	$\dfrac{\alpha}{\mathcal{I}}$	$\dfrac{\beta}{\sim\mathcal{I}^4}$
6	0	BC2	-0.26667	-0.3432	-0.457	$v_0(\mathcal{I},x_{00})$	0.50	$\eta_0(\mathcal{I},x_{00})$	-1.05	0.835
			-0.26667	-0.3667	-0.469	$\mathcal{M}_{BC2}^0$	0.50		-1.07	1.00
6	0	BC23	0	-0.058775	-0.115	$v_0(\mathcal{I},x_{00})$-0.31		0.55		
			0	-0.08229	-0.127	$\mathcal{M}_{BC2}^0$$-0.339$		0.496		
6	±1	BC2	0.13333	-0.110295	0.07625	$v_{\pm1}(\mathcal{I},x_{00})$	0.0425	$\eta_\pm(\mathcal{I},x_{00})$	0.55	0.4
			0.13333	-0.1260	0.0778	$\mathcal{M}_{BC2}^0$	0.0415		0.533	0.397
6	±1	BC23	0.26667	0.10304	0.11875	$v_{\pm1}(\mathcal{I},x_{00}) + 0.02$	0.0775	$\eta'_\pm(\mathcal{I},x_{00})$	1.	0.35
			0.26667	0.08737	0.120	$\mathcal{M}_{BC2}^0+0.0116$	0.0830		1.07	0.361
10	0	BC2	-0.44444	-0.95345	-2.10	$v_0(\mathcal{I},x_{00})$	4.25	$\eta_0(\mathcal{I},x_{00})$	-1.8	3.5
			-0.44444	-1.0187	-2.17	$\mathcal{M}_{BC2}^0$	3.86		-1.79	5.47
10	0	BC23	0	-0.16325	0.53	$v_0(\mathcal{I},x_{00})$-2.2		-1.75		
			0	-0.2286	-0.589	$\mathcal{M}_{BC2}^0$$-2.38$		1.59		
10	±1	BC2	0.22222	-0.3063725	0.3525	$v_{\pm1}(\mathcal{I},x_{00})$	0.305	$\eta_\pm(\mathcal{I},x_{00})$	0.95	0.89
			0.22222	-0.3499	0.360	$\mathcal{M}_{BC2}^0$	0.320		0.889	0.822
10	±1	BC23	0.44444	0.286235	0.548	$v_{\pm1}(\mathcal{I},x_{00}) + 0.001$	0.53	$\eta'_\pm(\mathcal{I},x_{00})$	1.75	0.9
			0.44444	0.2427	0.558	$\mathcal{M}_{BC2}^0$$-0.0472$	0.640		1.78	0.725
20	0	BC2	-0.88889	-3.815	-16.5	$v_0(\mathcal{I},x_{00})$	80.	$\eta_0(\mathcal{I},x_{00})$	-3.5	45.
			-0.88889	-4.075	-17.4	$\mathcal{M}_{BC2}^0$	61.7		-3.56	82.6
20	0	BC23	0	-0.653	-4.0	$v_0(\mathcal{I},x_{00})$-28.		20.		
			0	-0.914	-4.71	$\mathcal{M}_{BC2}^0$$-27.8$		20.4		
20	±1	BC2	0.44444	-1.22536	2.804	$v_{\pm1}(\mathcal{I},x_{00})$	4.475	$\eta_\pm(\mathcal{I},x_{00})$	2.335	11.6
			0.44444	-1.400	2.88	$\mathcal{M}_{BC2}^0$	5.12		1.78	8.16
20	±1	BC23	0.88889	1.14545	4.323	$v_{\pm1}(\mathcal{I},x_{00}) - 0.875$	7.0	$\eta'_\pm(\mathcal{I},x_{00})$	3.5	10.5
			0.88889	0.9707	4.46	$\mathcal{M}_{BC2}^0$$-1.47$	10.2		3.56	20.7

multichannel or the single-channel treatments proves that, for the considered light intensities, the adiabatic potential $V_{nad}^m(x)$ represents well the effective potential in the *p* wave. More importantly, it corroborates the separation of the expansion terms of $\mathcal{M}(x_{max})$ into two types [see Eqs. (A3) and (A4)]. The first type depends only on the asymptotic potential through the multipolar coefficients c_p and the coefficient c_{3f} for BC23 conditions. Among the second type, we encounter the constant coefficient $v_m(\mathcal{I}, x_{00})$, which depends on x_{00} and is similar to the parameter $\mathcal{M}_0$ of the analytical approach. In fact, the constants $v_m(\mathcal{I}, x_{00})$ obtained with the BC23 and BC2 boundary conditions are equivalent and differ simply by the known quantity $\Delta\mathcal{M}^0$ [Eq. (11)]. In addition, we have carefully verified that, when the light intensity tends to zero and the dipolar interaction becomes negligible, both $\mathcal{M}_0^{BC2}$ and $\mathcal{M}_0^{BC23}$ approach the standard field-free scattering volume.

Let us emphasize that the divergent contributions to $\mathcal{M}(x)$, which are proportional to x^2, x, and $\ln(x)$, arise from interactions that asymptotically decrease as $1/x^3$, $1/x^4$, and $1/x^5$. In contrast, the van der Waals interaction occurs (to leading order) in the term proportional to $1/x$ in the expansion of $\mathcal{M}(x)$. This is in agreement with the fact that the scattering volume can be defined in the standard way for long-range

potentials decreasing rapidly at least as $1/x^6$. For $\mathcal{M}_0$, a direct comparison between the numerical and analytical results is not possible. In the analytical Levy-Keller model, $\mathcal{M}_0$ appears as integration constant in the solution of Eq. (A2a). It could, in principle, be obtained if the value of $\mathcal{M}(x)$ is known at a sufficiently small x_b value ($x_b \ll 1$). However, since there is no explicit expression for this short-range boundary condition, it does not provide a means to determine $\mathcal{M}_0$. Therefore, this boundary condition at small x_b will be determined from numerical calculations in which all the interactions present at $x < x_b$ are introduced, whereas the asymptotic Hamiltonian Eq. (4) explicitly accounts for the interactions occurring at $x > x_b$. In the numerical approach, $\mathcal{M}_0$ is well determined provided that the number of channels n is sufficiently large to ensure convergence, as is shown in Sec. III B. The boundary condition at x_b plays a role very similar to the parameter t_0 in Eq. (9).

B. Dependence of the scattering volume on field-free *s*-wave scattering length and light intensity

For a given light intensity, the *p*-wave scattering volume depends only on the field-free *s*-wave scattering length, or
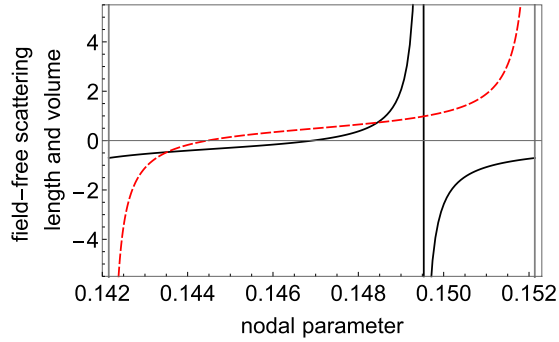
FIG. 1. Field-free *s*-wave scattering length (red dashed line) and field-free standard *p*-wave scattering volume (black solid line) as a function of the nodal parameter x_{00} (r.u. units are used). The gray vertical lines indicate the limits of the quasiperiod of the variation of the field-free *s*-wave scattering length associated with the seventh node (counted from outside) of the field-free *s*-wave threshold wave function. To each collision pair corresponds a particular value of the nodal parameter.

FIG. 2. Field-dressed *p*-wave scattering volume for $m = 0$ (upper panel) and $|m| = 1$ (lower panel) as a function of the nodal parameter x_{00} calculated for $n = 1$ (green dashed line), $n = 2$ (blue dotted line), $n = 3$ (red dot-dashed line) and $n = 4$ (black solid line) channels (r.u. units are used). The non-resonant light intensity is $\mathcal{I} = 6$ r.u. The resonances labeled by $\widetilde{\ell}$ correspond to a bound state at threshold with a dominant ℓ-contribution in its wave function. The vertical gray lines correspond to an infinite *s*-wave scattering length.

on the nodal parameter x_{00}, and captures all effects of the short-range interactions. We recall here that, as soon as the *s*-wave scattering length of a colliding pair is known, we can fix a suitable x_{00} for modeling the system using the asymptotic model [14,17]. Figure 1 shows the field-free *s*-wave scattering length and field-free *p*-wave scattering volume defined in the standard way versus x_{00}. In the absence of the nonresonant light, we use the ordinary definition of the scattering volume in Eq. (5) because the anisotropic $1/x^3$ term in the asymptotic Schrödinger Eq. (4) vanishes. Furthermore, there is no channel coupling and the single-channel approximation becomes exact. The range for x_{00} in Fig. 1, $x_{00} \in [0.142\,152, 0.152\,135]$ r.u., corresponds to one quasiperiod of the *s*-wave scattering length varying from $-\infty$ to $+\infty$. The divergences of the *s*-wave scattering length, which correspond to the contact interaction becoming infinite, are experimentally important since they represent a resonant situation with an $\ell = 0$ bound state at threshold, and are correlated to a large value of the partial *s*-wave cross section just above threshold [9,27]. The *p*-wave scattering volume also displays a singularity within this x_{00} range, with an $\ell = 1$ bound state at threshold, accompanied by a threshold shape resonance with asymmetrical profile in the partial *p*-wave cross section. The position and width of the singularities of the scattering length and scattering volume are completely different. This has been observed before for a truncated x^{-6} potential, with a repulsive wall at the position $x_0 \to 0_+$ [28], a simple model that predicts the *s*-wave scattering lengths corresponding to divergences of the scattering parameters in Eq. (5) in any partial ℓ wave. In particular, the field-free resonances ℓ and $\ell' = \ell + 4q$ (q integer) were found to be degenerate [28]. For the studied x_{00} range, our asymptotic model predicts that the field-free $\ell = 1$ scattering volume diverges at $x_{00} = 0.1495$ r.u., i.e., for the field-free scattering length $a = 0.9668$ r.u. (see also Ref. [17]), instead of the universal value 0.96 r.u. [28]. Similarly, the $\ell = 3$ field-free standard scattering volume, not shown in Fig. 1, diverges for $x_{00} = 0.1447$ r.u., i.e., for $a = 0.056\,51$ r.u., instead of the universal value $a = 0$ r.u. given in Ref. [28]. The re-
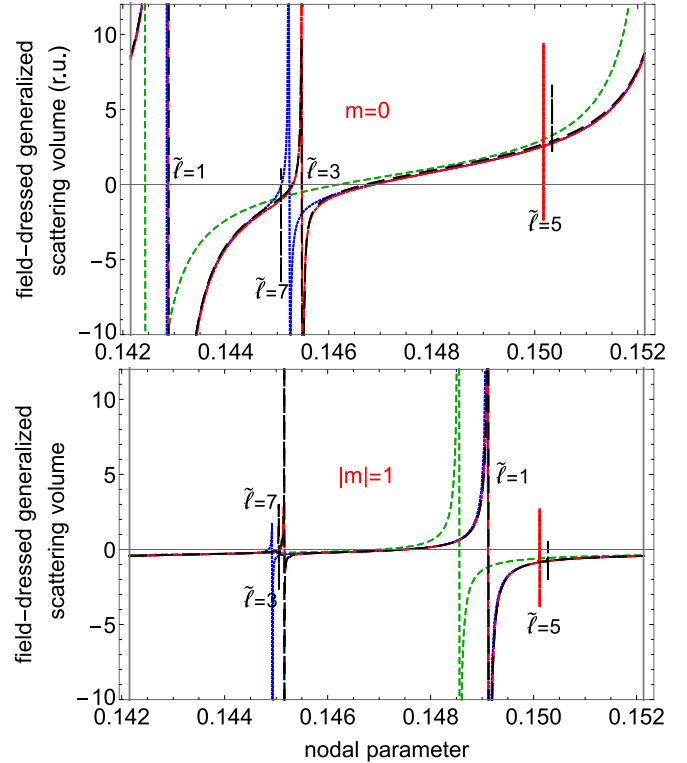
sults of Ref. [28] differ from those obtained by the nodal method due to the quasiperiodicity in the variation of the scattering length with $1/x_{00}^2$ which becomes more exact as x_{00} decreases [29].

We now analyze the field-dressed scattering volume as a function of x_{00} for $m = 0$ and ± 1 at a rather weak intensity $\mathcal{I} = 6$ r.u. in Fig. 2. Note that the nonresonant field interaction removes the m degeneracy. For the single-channel model $n = 1$ and $m = 0$, the field-dressed scattering volume diverges at $x_{00} = 0.1427$ r.u. in the top panel of Fig. 2, which is shifted from the field-free position $x_{00} = 0.1497$ r.u. in Fig. 1. This large shift in x_{00}, $\Delta x_{00} \sim 0.007$ r.u., shows the high sensitivity of the resonance on the nonresonant field intensity, due to the low rotational barrier for $\ell = 1$. By increasing the number of channels to $n = 2$, the $\ell = 1$, $m = 0$ resonance is slightly shifted toward higher x_{00} values, up to $x_{00} \sim 0.1432$ r.u. This is due to a small contribution of the $\ell = 3$ channel to the bound-state wave function labeled by $\widetilde{\ell} = 1$. For $\mathcal{I} = 6$ r.u., the different channels are weakly coupled so that the bound states $\widetilde{\ell}$ are clearly characterized by their dominant ℓ-wave contribution. The position of the $\widetilde{\ell} = 1$ resonance slightly varies with increasing n, and is stabilized for $n \geqslant 3$. For the $n = 2$ calculation, the scattering volume shows an additional singularity at $x_{00} = 0.1452$ r.u. associated with the occurrence

of a bound state at threshold with dominant $\ell = 3$ weight. As expected, the position of the field-dressed $\widetilde{\ell} = 3$ resonance is close to the field-free one $x_{00} = 0.1447$ r.u., the small shift $\Delta x_{00} < 0.005$ r.u. is due to the higher rotational barrier. For $n = 3$, another singularity associated with a $\widetilde{\ell} = 5$ bound state occurs around $x_{00} = 0.150$ r.u., and is very close to the field-free $\ell = 1$ resonance shown in Fig. 1. By using four channels, a $\widetilde{\ell} = 7$ resonance appears at $x_{00} \approx 0.145$ r.u., very close to the $\widetilde{\ell} = 3$ one. Indeed, by increasing the number of channels, the predicted degeneracy of the $\widetilde{\ell}$ and $\widetilde{\ell} + 4$ resonances [28] becomes manifest.

We analyze now the field-dressed resonances with $|m| = 1$ shown in the bottom panel of Fig. 2. A comparison with the field-dressed $m = 0$ resonances shows significant differences. In the $n = 1$ channel model, the $|m| = 1$ resonance position is $x_{00} = 0.1486$ r.u., suffering a shift, $\Delta x_{00} = 0.0009$ r.u., smaller than the one we encounter for the $|m| = 0$ resonance. Furthermore, the field-dressed $|m| = 1$ resonance is much narrower than the $m = 0$ one. This is ascribed to the effective potentials being asymptotically attractive (repulsive) for $m = 0$ ($|m| = 1$), the latter having a $1/x^3$ contribution two times smaller (see Table I). By increasing the number of channels, additional resonances with $|m| = 1$ and $\ell \geqslant 3$ appear. This demonstrates that, for these resonances, the strength of the channel mixing is approximately independent of m. Indeed, as ℓ increases, the resonance positions become almost m independent since they are essentially governed by the height and width of the rotational potential barriers.

Let us emphasize that the presence of a divergence of the scattering volume at x_{00} is linked to the appearance of a shape resonance at threshold, as we have verified. The shape resonance is due to tunneling through the rotational barrier and results in an asymmetric profile in the cross section. It destroys the universal character of dipolar scattering at ultracold temperatures which is characterized by partial wave cross sections which are proportional to $\mathcal{D}^2$ and are independent of collision energy.

At the rather low intensity $\mathcal{I} = 6$ r.u., the calculation of the field-dressed resonance $\widetilde{\ell}$ is almost converged when the multichannel model includes up to the $\ell' = \ell + 2$ channel, which corresponds to a model including $n \geqslant (\ell + 3)/2$ channels. In contrast, a larger number of channels are needed for much higher intensities or for dipolar partners coupled by strong dipole-dipole interaction $\mathcal{D}$. For instance, in Ref. [23] more than 30 channels are needed to describe the scattering cross sections of aligned dipolar molecules at ultracold collision energies. Indeed, collisions between KRb (respectively RbCs) molecules with equivalent dipole length $\mathcal{D} \sim 5700\,a_0$ (respectively $47\,000\,a_0$) and van der Waals length $\sigma \sim 140\,a_0$ (respectively $180\,a_0$) correspond to collisions in a strong nonresonant light with very high intensity $\mathcal{I} = 240$ r.u. (respectively 1600 r.u.).

IV. CONCLUSIONS

The standard definition of the *p*-wave scattering volume is known to diverge for $1/R^3$ interactions, which appear for atoms in a nonresonant light or for the dipole-dipole scattering between ultracold atoms or molecules. In this work, we have defined a generalized *p*-wave scattering volume

for two trapped ultracold atoms in nonresonant light. To this end, we have employed an asymptotic model [14,17], based on the fact that ultracold collisions are dominated by long-range forces. The short-range interactions are taken into account by the nodal parameter, which is fixed once the field-free *s*-wave scattering length is known. Note that when the light intensity tends to zero, the field-dressed *p*-wave scattering volume approaches the standard field-free scattering volume.

In detail, we have deduced the analytical expression of the *p*-wave component of the threshold wave function from the two-potential approach developed by Levy and Keller [16] in a single-channel approximation. For large R, this radial wave function expresses as a linear combination of R^2 and $1/R$ the free spherical wave solutions. The latter term is multiplied by a R-dependent factor similar to the tangent of the local phase shift, but asymptotically diverging. We have shown that this factor includes a constant term capturing the nonuniversal part of the short-range contributions to dipolar scattering and generalizing, with the proper dimension, the standard definition of the scattering volume. In numerical multichannel calculations, the *p*-wave scattering volume is obtained by fitting the asymptotic behavior of the *p*-wave component of the threshold wave function to the analytical expansion.

The asymptotic model depends only on the nodal parameter x_{00}, which is fixed once the field-free *s*-wave scattering length of the collision partners is known [17]. In absence of nonresonant light, we have analyzed the dependence of the field-free *p*-wave scattering volume on this parameter x_{00}, which is significantly different from the *s*-wave scattering length dependence. The *p*-wave scattering volume also displays one singularity in the x_{00} range where the *s*-wave scattering length changes from $-\infty$ to $+\infty$. This is in line with earlier predictions [28]. The singularity is caused by the appearance of a $\ell = 1$ bound state at threshold. In presence of nonresonant light, the original *p*-wave singularity is shifted and, more remarkably, additional singularities appear. This is due to the field-dressed *p*-wave function containing contributions from additional field-free partial waves for which a bound state at threshold appears.

Instead of universal nodal lines with a single nodal parameter introduced in this paper, it is possible to consider nodal lines with energy ℓ and also intensity (equivalently dipole strength) dependence adjusted to a real pair of atoms [17,18]. In this case, the short-range interactions are more precisely accounted for and an accurate prediction of the near threshold resonances becomes possible. This description is equivalent to those introducing a regularized zero-range potential, the so-called contact interaction, with infinitely many terms [25], but is probably more tractable. In addition, multipolar ultracold collisions can be studied, in a straightforward extension of this work to the nonzero energy regime, as it has been done in previous studies devoted to the analysis of shape resonances [17,18,30].

In the following paper (Paper II [15]), we will use the method developed here to control the scattering volume using nonresonant light. This is an extension of our previous work on controlling the *s*-wave scattering length [14].

APPENDIX A: TWO-POTENTIAL LEVY-KELLER APPROACH

1. Levy-Keller method

The two-potential method was proposed by Levy and Keller [16,20,32] to determine the single-channel wave function $u(x) \equiv u_\ell(x)$, which is the ℓ-wave solution of the Schrödinger Eq. (7) associated to the potential $V(x) \equiv V_\ell(x) = -c_3/x^3 - c_4/x^4 - c_5/x^5 - c_6/x^6$ [see Eq. (6)], with energy $\epsilon = k^2$. In this model a second potential $V_f(x)$ is introduced, leading to the definition of a "reference" pair of functions $(\varphi(x), \psi(x))$. They are linearly independent solutions of the Schrödinger equation of the potential $V_f(x)$ at the same energy ϵ and for the same ℓ. This ℓ-wave solution $u(x)$ is written as a linear x-dependent combination of the reference functions

$$u(x) = \mathcal{A}(x)[\varphi(x) - \psi(x)\mathcal{M}(x)], \quad \text{(A1a)}$$

with the imposed condition

$$\frac{du(x)}{dx} = \mathcal{A}(x)\left(\frac{d\varphi(x)}{dx} - \frac{d\psi(x)}{dx}\mathcal{M}(x)\right). \quad \text{(A1b)}$$

In the expression (A1a), $\mathcal{A}(x)$ is a global amplitude, and $\mathcal{M}(x)$ the relative amplitude of $\varphi(x)$ and $\psi(x)$. $\mathcal{M}(x)$ plays the role of $\tan\delta(x)$, with $\delta(x)$ being the local phase shift describing the collisional partial waves in terms of spherical Bessel and Neumann functions.

To solve Eq. (A1), we first eliminate the global amplitude $\mathcal{A}(x)$ in Eq. (A1a) by using the radial Schrödinger equations satisfied by $u(x)$ and by the pair $(\varphi(x), \psi(x))$, and the imposed condition (A1b). We derive the following equation for the relative amplitude:

$$\frac{d\mathcal{M}(x)}{dx} = -\frac{V(x) - V_f(x)}{W}[\varphi(x) - \psi(x)\mathcal{M}(x)]^2, \quad \text{(A2a)}$$

with W being the Wronskian of the reference pair, $W = \varphi(x)\psi'(x) - \varphi'(x)\psi(x)$. The integration of this differential equation introduces a constant $\mathcal{M}_0$, which may depend on the reference pair. In a second step, we obtain the differential equation for the logarithmic derivative of $\mathcal{A}(x)$:

$$\frac{d\ln(\mathcal{A}(x))}{dx} = -\frac{V(x) - V_f(x)}{W}\psi(x)[\varphi(x) - \psi(x)\mathcal{M}(x)], \quad \text{(A2b)}$$

which is integrated imposing the boundary condition $\mathcal{A}(x) \to 1$ for $x \to \infty$. Once $\mathcal{A}(x)$ and $\mathcal{M}(x)$ are determined, the solution $u(x)$ is obtained. We emphasize that, obviously, $u(x)$ does not depend on the choice of the second potential $V_f(x)$ nor on the reference pair. If $V(x)$ expresses as a multipolar expansion (6), an analytical expression for the asymptotic form of $u(x)$ can be obtained for energy $\epsilon > 0$ when free spherical waves are chosen as reference functions or at threshold $\epsilon = 0$ for different reference functions.

In summary, the Levy-Keller method first computes $\mathcal{M}(x)$, which is related to the local phase shift, and the amplitude $\mathcal{A}(x)$ is independently obtained in a second step, after introducing an arbitrary constant $\mathcal{M}_0$. In contrast, in the extensively used phase-amplitude method pioneered by Milne [33], the amplitude satisfies a nonlinear equation that is integrated first and the phase is calculated in a second step. Thus, the pair of functions amplitude and phase, which parametrize the wave function, are not unique and does not necessarily lead to the determination of the scattering parameters in Eq. (5). Note that a direct integral representation for scattering phase shifts, based on a modified version of Milne's approach, has been recently proposed [34].

Note also that the asymptotic solution of Eq. (7) could be constructed using perturbation theory, as done by Hinckelmann and Spruch with another formulation of the two-potential approach [20]. For the long-range part $x > d$, they consider a single multipolar potential $V(x) = -c_{pf}/x^q$, and for the short-range one $x < d$, an unknown potential characterized at $x = d$ by a phase $\delta_\ell(k, x = d)$ such as $\tan[\delta_\ell(k, x = d)]$ increases as $k^{2\ell+1}$ at low energy. For $x > d$, the phase of the wave function is obtained by treating the external part of $V(x)$ to first order of perturbation theory, the zeroth order consisting of free spherical waves. This procedure is analogous to the Levy-Keller approach with the reference pair BC2k and $V_f(x) = 0$ (see Table II), and determining $\mathcal{M}(x)$ by first-order perturbation theory.

2. Reference pairs

The analytical pairs $(\varphi(x), \psi(x))$ used in this work to obtain analytical solutions $u(x)$ of the Schrödinger Eq. (7) by the Levy-Keller method are presented in Table II. These reference functions depend on the energy and on the chosen potential $V_f(x)$. They are labeled according to the imposed asymptotic behavior, i.e., the boundary conditions (BC). Whereas the wave function $u(x)$ does not depend on the reference pair, the relative amplitude $\mathcal{M}(x)$ and the global amplitude $\mathcal{A}(x)$ depend *a priori* on the chosen $\varphi(x)$ and $\psi(x)$.

For positive energy $\epsilon = k^2 > 0$, we use the reference pair labeled by BC2k, which corresponds to the spherical Bessel and Neumann functions describing free spherical waves. For vanishingly small wave number k and not too large distance, $x \ll 1/k$, such that $kx \to 0$, the reference functions behave as $\varphi(x) \propto (kx)^{\ell+1}$ and $\psi(x) \propto (kx)^{-\ell}$.

Considering the solutions at threshold, i.e., $k = 0$, the reference pair BC2 corresponds to the partial waves for free motion, i.e., $V_f(x) = 0$, with functions $\varphi_{BC2}(x) = x^{\ell+1}$ and $\psi_{BC2}(x) = 1/x^\ell$. The p-wave pair of BC23 functions $(\varphi_{BC23}(x), \psi_{BC23}(x))$ correspond to the solutions at threshold of the potential $V_f(x) = -c_{3f}/x^3$ with $c_{3f} > 0$.

These analytical functions are proportional to the Bessel functions of second kind $Y_3(\sqrt{4c_{3f}/x})$ and first kind $J_3(\sqrt{4c_{3f}/x})$ (see Table II), and have been used for $\ell \geqslant 3$ in Ref. [31].

For the three sets of reference functions with $\ell = 1$, $\mathcal{M}(x)$ is the value in reduced units of a quantity that has dimension of volume.

3. Analytic expansion at threshold for *p* waves of $\mathcal{M}(x)$, $\mathcal{A}(x)$, and $u(x)$

For the potential $V(x)$ [Eq. (6)] and a chosen pair of reference functions see (Table II), the asymptotic expansion of $\mathcal{M}(x)$, solution of Eq. (A2a), is obtained analytically by identifying the coefficients of the x^q and $\ln(x)/x^q$ terms (see Sec. II E for more details). This method does not allow the determination of the constant term $\mathcal{M}_0$, which does not depend on the asymptotic properties of the Hamiltonian Eq. (7). When the nodal line technique is used, $\mathcal{M}_0$ depends only on the nodal parameter x_{00}.

Using the BC2 reference pair $(x^2, 1/x)$, one obtains

$$\mathcal{M}_{\text{BC2}}(x) = -\frac{c_3}{6}x^2 - \left(\frac{c_3^2}{9} + \frac{c_4}{3}\right)x - \left(\frac{c_3^3}{12} + \frac{c_3 c_4}{3} + \frac{c_5}{3}\right)\ln(x) + \mathcal{M}_0^{\text{BC2}} + \left(\frac{c_3^4}{18} + \frac{2c_3^2 c_4}{9} + \frac{2c_3 c_5}{9}\right)\frac{\ln(x)}{x}$$

$$+ \left(\frac{11c_3^4}{162} + \frac{37c_3^2 c_4}{108} + \frac{2c_4^2}{9} + \frac{c_3 c_5}{3} + \frac{c_6}{3} - \frac{2c_3\mathcal{M}_0^{\text{BC2}}}{3}\right)\frac{1}{x} + \cdots. \tag{A3}$$

For the BC23 reference functions associated with the potential $V_f = -c_{3f}/x^3$ $(c_{3f} > 0)$, it yields

$$\mathcal{M}_{\text{BC23}}(x) = -\frac{c_3 - c_{3f}}{6}x^2 - \left(\frac{(c_3 - c_{3f})^2}{9} + \frac{(c_3 - c_{3f})c_{3f}}{3} + \frac{c_4}{3}\right)x$$

$$- \left(\frac{c_3^3 - c_f^3}{12} + \frac{c_3 c_4}{3} + \frac{c_5}{3}\right)\ln(x) + \mathcal{M}_0^{\text{BC23}} + (c_3 - c_{3f})\left(\frac{c_3^3}{18} + \frac{2c_3 c_4}{9} + \frac{2c_5}{9}\right)\frac{\ln(x)}{x}$$

$$+ \left[(c_3 - c_{3f})\left(\frac{11c_3^3}{162} + \frac{c_3^2 c_{3f}}{72} + \frac{c_3 c_{3f}^2}{135} + \frac{491c_{3f}^3}{3240} + \frac{5c_3 c_4}{54} - \frac{7c_{3f} c_4}{108}\right)\right.$$

$$\left. + \frac{2c_4^2}{9} + \frac{c_3 c_5}{3} + \frac{c_6}{3} - \frac{(c_3 - c_{3f})c_{3f}^3 \gamma}{9} - \frac{(c_3 - c_{3f})c_{3f}^3 \ln(c_{3f})}{18} - \frac{2(c_3 - c_{3f})}{3}\mathcal{M}_0^{\text{BC23}}\right]\frac{1}{x} + \cdots \tag{A4}$$

with γ being the Euler constant.

When c_3 is positive, it is possible to account entirely in the reference functions for the $-c_3/x^3$ attractive contribution to the potential $V(x)$ by setting $c_{3f} = c_3$. The expression of $\mathcal{M}_{\text{BC23}}(x)$ is then particularly simple because the terms x^2 and $\ln(x)/x$ disappear, and the x term depends only on c_4. Furthermore, for $c_{3f} = c_3$, the $1/x$ term does not have contributions from $\mathcal{M}_0^{\text{BC23}}$ and $\ln(c_3)$ nor from c_3^4. This simple case $c_{3f} = c_3$ is used in the study of the $\ell = 1$ and $m = 0$ states for which the adiabatic approximation to the effective potential in the *p* channel is asymptotically attractive (see Table I). For the $\ell = 1$ and $|m| = 1$ states, the adiabatic *p*-wave potential $V_{nad}^{|m|=1}(x)$ is repulsive ($c_3 < 0$ see Table I) and $c_{3f} = -c_3$ is used in BC23 to ensure real reference functions and real $\mathcal{M}(x)$. The asymptotic form for $\mathcal{M}_{\text{BC23}}^{c_{3f}=-c_3}(x)$ is then given by Eq. (A4).

For a given potential $V(x)$ [Eq. (6)], the asymptotic expansions of $\mathcal{M}_{\text{BC2}}(x)$ and $\mathcal{M}_{\text{BC23}}(x)$ depend on the multipolar coefficients c_p of $V(x)$ and on the c_{3f} coefficient defining the BC23 reference pair. Furthermore, they introduce *a priori* different constant coefficients $\mathcal{M}_0^{\text{BC2}}$ and $\mathcal{M}_0^{\text{BC23}}$, which take into account the contribution of the inner part of the potential $V(x)$ not involved in the derivation of Eqs. (A3) and (A4). This constant $\mathcal{M}_0$ is the x-independent term in $\mathcal{M}(x)$ and also appears in some x-dependent terms. For instance, the coefficient of the term $1/x$ can be expressed as $\eta = \alpha \mathcal{M}_0 - \beta$, where α and β only depend on the multipolar coefficients c_p of $V(x)$ and on c_{3f}. For the reference pair BC23 and $c_{3f} = c_3$, the coefficient of $1/x$ is independent on x_{00} and only depends on $V(x)$. The calculation of the difference $\Delta\mathcal{M}_0 = \mathcal{M}_0^{\text{BC23}} - \mathcal{M}_0^{\text{BC2}}$ [whose result is given in Eq (11)] is presented below.

Using these analytical asymptotic expansions of $\mathcal{M}(x)$, we integrate Eq. (A2b), and impose the asymptotic condition $\mathcal{A}(x) \rightarrow 1$ for $x \rightarrow \infty$, to obtain the analytical expressions of $\mathcal{A}(x)$. For the BC2 and BC23 reference pairs, we encounter the following analytical expressions of $\mathcal{A}(x)$:

$$\mathcal{A}_{BC2}(x) = 1 + \frac{c_3}{3}\frac{1}{x} + \left(\frac{c_3^2}{12} + \frac{c_4}{6}\right)\frac{1}{x^2} + \left(\frac{c_3^3}{36} + \frac{c_3 c_4}{9} + \frac{c_5}{9}\right)\frac{1}{x^3} + \cdots \tag{A5}$$

$$\mathcal{A}_{BC23}(x) = 1 + \frac{c_3 - c_{3f}}{3x} + \left(\frac{(c_3 - c_{3f})^2}{12} + \frac{c_{3f}(c_3 - c_{3f})}{24} + \frac{c_4}{6}\right)\frac{1}{x^2}$$

$$+ \left(\frac{(c_3 - c_{3f})^3}{36} + \frac{(c_3 - c_{3f})^2 c_{3f}}{24} + \frac{(c_3 - c_{3f})c_{3f}^2}{60} + \frac{c_4(c_3 - c_{3f})}{9} + \frac{c_4 c_{3f}}{36} + \frac{c_5}{9}\right)\frac{1}{x^3} + \cdots. \tag{A6}$$

For $c_{3f} = c_3$, the expression for $\mathcal{A}_{\text{BC23}}(x)$ is simpler because the $1/x$ contribution disappears, and the $1/x^2$ and $1/x^3$ terms depend only on c_4, and on c_5 and $c_4 c_3$, respectively.

Using these analytical expressions of $\mathcal{M}(x)$ and $\mathcal{A}(x)$, we obtain from Eq. (A1a) the following asymptotic expansions of the threshold p-wave function $u(x)$:

$$u_{\text{BC2}}(x) = x^2 + \frac{c_3}{2}x + \left(\frac{c_3^2}{4} + \frac{c_4}{2}\right) + \left(\frac{c_3^3}{12} + \frac{c_3 c_4}{3} + \frac{c_5}{3}\right)\frac{\ln(x)}{x} + \left(\frac{17c_3^3}{216} + \frac{c_3 c_4}{4} + \frac{c_5}{9} - \mathcal{M}_0^{\text{BC2}}\right)\frac{1}{x}$$

$$- \left(\frac{c_3^4}{48} + \frac{c_3^2 c_4}{12} + \frac{c_3 c_5}{12}\right)\frac{\ln(x)}{x^2} - \left(\frac{79c_3^4}{1728} + \frac{11c_3^2 c_4}{48} + \frac{c_4^2}{8} + \frac{c_6}{4} + \frac{37c_3 c_5}{144} - \frac{c_3 \mathcal{M}_0^{\text{BC2}}}{4}\right)\frac{1}{x^2} + \cdots , \quad \text{(A7)}$$

$$u_{\text{BC23}}(x) = x^2 + \frac{c_3}{2}x + \left(\frac{c_3^2}{4} + \frac{c_4}{2}\right) + \left(\frac{c_3^3}{12} + \frac{c_3 c_4}{3} + \frac{c_5}{3}\right)\frac{\ln(x)}{x}$$

$$+ \left[\frac{17c_3^3}{216} + \frac{c_3 c_4}{4} + \frac{c_5}{9} - \mathcal{M}_0^{\text{BC23}} - \left(\frac{2}{9}c_4 + \frac{11}{144}c_3^2\right)c_{3f} - \frac{c_3 c_{3f}^2}{24} + \left(\frac{83}{432} - \frac{\gamma}{6} - \frac{\ln(c_{3f})}{12}\right)c_{3f}^3\right]\frac{1}{x}$$

$$- \left(\frac{c_3^4}{48} + \frac{c_3^2 c_4}{12} + \frac{c_3 c_5}{12}\right)\frac{\ln(x)}{x^2} - \left\{\frac{79c_3^4}{1728} + \frac{11c_3^2 c_4}{48} + \frac{c_4^2}{8} + \frac{c_6}{4} + \frac{37c_3 c_5}{144}\right.$$

$$\left. + \frac{c_3}{4}\left[-\mathcal{M}_0^{\text{BC23}} - \left(\frac{2}{9}c_4 + \frac{11}{144}c_3^2\right)c_{3f} - \frac{c_3 c_{3f}^2}{24} + \left(\frac{83}{432} - \frac{\gamma}{6} - \frac{\ln(c_{3f})}{12}\right)c_{3f}^3\right]\right\}\frac{1}{x^2} + \cdots . \quad \text{(A8)}$$

Let us recall that the wave function $u(x)$ does not depend on the chosen reference pair. Thus, comparing $u_{\text{BC2}}(x)$ and $u_{\text{BC23}}(x)$, i.e., (A7) and (A8), the coefficients of the $1/x$ and $1/x^2$ terms are equal only if the constants $\mathcal{M}_0^{\text{BC2}}$ and $\mathcal{M}_0^{\text{BC23}}$ are related by Eq. (11), which only involves the multipolar constants c_p of $V(x)$ and the coefficient c_{3f} defining the BC23 reference pair. We have verified that relation (11) ensures the equality of the coefficients multiplying $1/x^3$, $1/x^4$, $1/x^5$, $\ln(x)/x^3$, $\ln(x)/x^4$, and $\ln(x)/x^5$ in the wave functions $u_{\text{BC2}}(x)$ and $u_{\text{BC23}}(x)$. For $c_{3f} \to 0$, the reference pairs BC23 and BC2 become identical and $\mathcal{M}_0^{\text{BC23}} \to \mathcal{M}_0^{\text{BC2}}$.

APPENDIX B: MULTICHANNEL DETERMINATION OF $\mathcal{M}_0$

1. Multichannel calculations

The nodal line technique presented in detail in Ref. [14] is used to numerically solve the asymptotic multichannel Schrödinger Eq. (4) in an n-channel model (odd ℓ values, $\ell = 1, 3, \ldots, 2n-1$). We expand the threshold wave functions $f(x, \theta, \phi)$ in terms of spherical harmonics and restrict the number of odd-parity partial waves to n, with $n = (\ell_{\max} - \ell_{\min} + 2)/2$ and $\ell_{\min} = 1 \leqslant \ell \leqslant \ell_{\max}$ with ℓ odd. The scattering volume is determined by choosing a particular p-wave physical threshold solution. We impose to this solution, written as the vector $\mathbf{z}^{j=1}(x)$, with n radial components $z_\ell^{j=1}(x)$, to decrease asymptotically in all channels $\ell \geqslant 3$, and to diverge only in the $\ell = 1$ channel. This solution is constructed from n particular pairs of solutions $(\mathbf{f}_+^j(x), \mathbf{f}_-^j(x))$ $(1 \leqslant j \leqslant n)$ with radial components $(f_{+,\ell}^j(x), f_{-,\ell}^j(x))$ in the different ℓ channels, and with imposed asymptotic forms. Each pair is associated with a particular channel $\ell = \ell_j$, with $\ell_{j=1} = 1$ and the asymptotic form of its component in this ℓ_j channel is imposed at $x_{\max}$ to be one of the analytical functions BC2 or BC23 defined for $k = 0$ in Table II. In other words, the asymptotic form in this channel is $\varphi(x) \propto x^{\ell_j+1}$ for $f_{+,\ell_j}^j(x)$

or $\psi(x) \propto 1/x^{\ell_j}$ for $f_{-,\ell_j}^j(x)$, whereas the components in the other channels $f_{\pm,\ell}^j(x)$, $\ell \neq \ell_j$, are vanishingly small. Thus, the asymptotic form of this solution in the $\ell = 1$ channel has to satisfy [cf. Eqs. (14) and (15) of Ref. [14]]

$$z_{\ell=1}^{j=1}(x) = f_{+,\ell=1}^{j=1}(x) - \sum_{j'=1}^{n} \overline{\mathbf{M}}_{j'}^{j=1}(x_{00}, x_{\max}) f_{-,\ell=1}^{j'}(x), \quad \text{(B1)}$$

where $f_{+,\ell=1}^{j=1}(x)$ increases asymptotically as x^2, whereas $f_{-,\ell=1}^{j'}(x)$ vanishes at least as $1/x^3$ for $j' \geqslant 2$ and as $1/x$ for $j' = 1$, i.e., they satisfy either the BC2 or the BC23 boundary conditions at $x_{\max}$ specified in Table II. For the boundary condition BC23, the potential $V_f(x) = -|c_3|/x^3$ is used to determine the initial value for the inward interaction of the pair $f_{\pm,\ell=1}^{j=1}(x_{\max})$, the adiabatic potential for p-wave being attractive (respectively repulsive) for $m = 0$ (respectively $|m| = 1$) (see Table I).

The coefficients $\overline{\mathbf{M}}_{j'}^{j=1}(x_{00}, x_{\max})$ in Eq. (B1) are determined by imposing to each radial ℓ component of $\mathbf{z}^{j=1}(x)$ to vanish at short range on what we call the nodal line x_{00}. The nodal line technique [18] replaces the interaction at very small distances $x < x_{00}$ by a repulsive wall in each channel at $x_0 \equiv x_0(\mathcal{E}, \ell, \mathcal{I})$ with $x_{00} = x_0(0, 0, 0)$ [35,36]. This nodal parameter x_{00} determines the position of ℓ-, energy-, and intensity-dependent repulsive walls $x_0(\mathcal{E}, \ell, \mathcal{I})$ in all channels, and thus contains in an effective way all information on the short-range interaction up to the nodal line. For more details on the choice of $x_0(\mathcal{E}, \ell, \mathcal{I})$, the reader is referred to Ref. [14].

The terms $\overline{\mathbf{M}}_{j'}^{j=1}(x_{00}, x_{\max})$ are x-independent constants, and depend on $x_{\max}$, the starting point of the inward integration, on the nodal parameter x_{00} and on the boundary conditions BC2 or BC23. At $x = x_{\max}$, we write

$$z_{\ell=1}^{j=1}(x_{\max}) \approx f_{+,\ell=1}^{j=1}(x_{\max}) - \mathcal{M}(x_{\max}) f_{-,\ell=1}^{j=1}(x_{\max}),$$

$$\text{(B2)}$$

replacing $\overline{\mathbf{M}}^{j=1}_{j'=1}(x_{00}, x_{\max})$ by $\mathcal{M}(x_{\max})$. If we identify

$$f^{j=1}_{+,\ell=1}(x_{\max}) = \varphi(x_{\max}),$$
$$f^{j=1}_{-,\ell=1}(x_{\max}) = \psi(x_{\max}), \tag{B3}$$

Eq. (B2) resembles the function $u(x)/\mathcal{A}(x)$ of the single-channel approximation (8), suggesting that $\mathcal{M}(x_{\max})$ plays a role similar to the tangent of the local phase shift in the p wave at the position $x_{\max}$.

2. Fits of the numerical $\mathcal{M}(x_{\max})$ to the Levy-Keller expansions

The coefficients of the terms x^2, x, $\ln(x)$, 1, $\ln(x)/x$, and $1/x$ [see Eq. (12)] in the expression of $\mathcal{M}(x)$ obtained from a fit of numerical multichannel calculations of $\mathcal{M}(x_{\max})$ for a large number of $x_{\max}$ values are presented in Table III. The analytical ones, obtained with the Levy-Keller approach using the asymptotic effective potential $V^m_{nad}(x)$ in the p wave (see Table I), are also presented. For fixed m, $\mathcal{I}$, and boundary conditions BC, the numerical and analytical coefficients are shown in the upper and lower lines, respectively, of the same cell in Table III.

We encounter coefficients independent of x_{00}, their numerical values are specified in Table III, whereas others depend on x_{00}. The coefficients of the constant and $1/x$ terms, labeled by the symbols $v_m(\mathcal{I}, x_{00})$ and $\eta_m(\mathcal{I}, x_{00})$, respectively, depend on x_{00} with a shape presenting several divergences (see Fig. 2). Note that for BC23 and $m = 0$, $\eta_m(\mathcal{I}, x_{00})$ is independent of x_{00}, and its value is given in Table III.

For given m and $\mathcal{I}$, the $v_m(\mathcal{I}, x_{00})$ of the BC2 and BC23 boundary conditions differ by a constant, which is independent of x_{00} and is listed in the first line of a BC23 cell in column 7. The corresponding analytical difference can be expressed in terms of c_3 and c_{3f} and its numerical value is reported in the second line of the same cell. The multichannel numerical values agree well with the estimates obtained in the single-channel approximation in Eq. (11). Similarly, for given m and $\mathcal{I}$, the coefficients $v_m(\mathcal{I}, x_{00})$ and $\eta_m(\mathcal{I}, x_{00})$ are related

by a linear transformation $\eta(\mathcal{I}, x_{00}) = v(\mathcal{I}, x_{00})\alpha - \beta$, with the α and β coefficients reported in cells of columns 10 and 11 of Table III. Here, we also find a good agreement between the fitted and single-channel approximation results reported in the same cell in the upper and lower lines, respectively.

The intensity dependence of the coefficients in the $\mathcal{M}(x_{\max})$ expansion are obtained from the single-channel formulas and the expansion of $V^m_{ad}(x)$. This dependence, indicated in the second line of the top cells of Table III, is reproduced by the numerical fits. At low intensity, the $\mathcal{I}/x^2_{\max}$ contribution prevails (column 4), whereas for increasing intensity the contribution of higher orders such as $\mathcal{I}^4 \times \ln(x_{\max})/x_{\max}$ (column 8) becomes important. The difference $\mathcal{M}^0_{BC23} - \mathcal{M}^0_{BC2}$ varies as $a\mathcal{I}^3 + b\ln(\mathcal{I})$ (column 7). For BC32 and $m = 0$, the coefficient of $1/x_{\max}$ varies as $1/3 + b'\mathcal{I}^4$ (column 9), the first term arising from the van der Waals interaction. The same dependence occurs for the factor β (column 11).

The numerical values obtained by fitting the multichannel $(n = 3)$ results agree well with the single-channel $(p$-wave) approximation coefficients derived using an adiabatic potential (cf. upper and lower lines in each cell of Table III). In particular, both calculations reproduce the classification of the coefficients into two types: the first one characteristic of the asymptotic p-wave potential, the other one accounting for the interactions at short distances. In addition, we emphasize that the values of $\mathcal{M}_0$ corresponding to the BC2 and BC23 boundary conditions are equivalent and are related by a general expression depending only on the asymptotic potential [see Eq. (11)].

The results from Table III justify the extraction from the multichannel calculations, or more precisely from the expansion of the divergent $\mathcal{M}(x_{\max})$ into powers of $1/x_{\max}$, a term independent of $x_{\max}$, $v_m(\mathcal{I}, x_{00})$. This quantity plays the same role as $\mathcal{M}_0$ in the single-channel approximation. Thus, as in the single-channel approximation, we introduce in the multichannel model a scattering volume given by $v_m(\mathcal{I}, x_{00})$, which characterizes low-energy collisions when the dynamics is governed by an anisotropic $1/x^3$ interaction.

[1] J. Dalibard, in *Proceedings of the International School of Physics "Enrico Fermi", Bose-Einstein Condensation in Atomic Gases*, edited by M. Inguscio, S. Stringari, and C.-E. Wieman (IOS Press, Amsterdam, 1999), Vol. 140, pp. 321–349.

[2] S. Giorgini, L. P. Pitaevskii, and S. Stringari, Rev. Mod. Phys. **80**, 1215 (2008).

[3] C. Chin, R. Grimm, P. Julienne, and E. Tiesinga, Rev. Mod. Phys. **82**, 1225 (2010).

[4] M. Theis, G. Thalhammer, K. Winkler, M. Hellwig, G. Ruff, R. Grimm, and J. H. Denschlag, Phys. Rev. Lett. **93**, 123001 (2004).

[5] S. Blatt, T. L. Nicholson, B. J. Bloom, J. R. Williams, J. W. Thomsen, P. S. Julienne, and J. Ye, Phys. Rev. Lett. **107**, 073202 (2011).

[6] R. Yamazaki, S. Taie, S. Sugawa, K. Enomoto, and Y. Takahashi, Phys. Rev. A **87**, 010704 (2013).

[7] M. Yan, B. J. DeSalvo, B. Ramachandhran, H. Pu, and T. C. Killian, Phys. Rev. Lett. **110**, 123201 (2013).

[8] T. F. O'Malley, L. Spruch, and L. Rosenberg, J. Math. Phys. **2**, 491 (1961).

[9] C. Joachain, *Quantum Collision Theory*, 3rd ed. (North-Holland, Amsterdam, 1983).

[10] H. R. Sadeghpour, J. L. Bohn, M. J. Cavagnero, B. D. Esry, I. I. Fabrikant, J. H. Macek, and A. R. P. Rau, J. Phys. B: At., Mol. Opt. Phys. **33**, R93 (2000).

[11] T.-O. Müller, Phys. Rev. Lett. **110**, 260401 (2013).

[12] M. Marinescu and L. You, Phys. Rev. Lett. **81**, 4596 (1998).

[13] B. Deb and L. You, Phys. Rev. A **64**, 022717 (2001).

[14] A. Crubellier, R. González-Férez, C. P. Koch, and E. Luc-Koenig, Phys. Rev. A **95**, 023405 (2017).

[15] A. Crubellier, R. González-Férez, C. P. Koch, and E. Luc-Koenig, following paper, Phys. Rev. A **99**, 032710 (2019).

[16] B. R. Levy and J. B. Keller, J. Math. Phys. **4**, 54 (1963).

[17] B. E. Londoño, J. E. Mahecha, E. Luc-Koenig, and A. Crubellier, Phys. Rev. A **82**, 012510 (2010).

[18] A. Crubellier, R. González-Férez, C. P. Koch, and E. Luc-Koenig, New J. Phys. **17**, 045020 (2015).

[19] L. Landau and E. Lifchitz, *Mécanique Quantique* (Editions Mir, Moscow, 1967).

[20] O. Hinckelmann and L. Spruch, Phys. Rev. A **3**, 642 (1971).

[21] R. Shakeshaft, J. Phys. B: At. Mol. Phys. **5**, L115 (1972).

[22] H. Friedrich, *Scattering Theory* (Springer, Berlin, 2016).

[23] J.-L. Bohn, M. Cavagnero, and C. Ticknor, New J. Phys. **11**, 055039 (2009).

[24] Y. Wang and C. H. Greene, Phys. Rev. A **85**, 022704 (2012).

[25] A. Derevianko, Phys. Rev. A **67**, 033607 (2003).

[26] Z. Idziaszek and T. Calarco, Phys. Rev. Lett. **96**, 013201 (2006).

[27] A. Messiah, *Mécanique Quantique* (Dunod, Paris, 1969), Vol. 1.

[28] B. Gao, Phys. Rev. A **80**, 012702 (2009).

[29] G. F. Gribakin and V. V. Flambaum, Phys. Rev. A **48**, 546 (1993).

[30] A. Crubellier, R. González-Férez, C. P. Koch, and E. Luc-Koenig, New J. Phys. **17**, 045022 (2015).

[31] M. J. Moritz, C. Eltschka, and H. Friedrich, Phys. Rev. A **63**, 042102 (2001).

[32] T. F. O'Malley, Phys. Rev. **134**, A1188 (1964).

[33] W. E. Milne, Phys. Rev. **35**, 863 (1930).

[34] D. Shu, I. Simbotin, and R. Côté, Phys. Rev. A **97**, 022701 (2018).

[35] A. Crubellier, O. Dulieu, F. Masnou-Seeuws, M. Elbs, H. Knöckel, and E. Tiemann, Eur. Phys. J. D **6**, 211 (1999).

[36] N. Vanhaecke, C. Lisdat, B. T'Jampens, D. Comparat, A. Crubellier, and P. Pillet, Eur. Phys. J. D **28**, 351 (2004).